

Inclusion-localised crystal-plasticity, dynamic porosity, and fast-diffusion pathway generation in zircon

Nicholas E. Timms^{a,*}, Steven M. Reddy^a, John D. Fitz Gerald^b, Leonard Green^c, Janet R. Muhling^d

^aDepartment of Applied Geology, Curtin University, GPO Box U1987, Perth, WA 6845, Australia

^bResearch School of Earth Sciences, Australian National University, Canberra 0200, Australia

^cAdelaide Microscopy, University of Adelaide, Adelaide, SA 5005, Australia

^dCentre for Microscopy, Characterisation and Analysis, University of Western Australia, Perth, WA 6009, Australia

ARTICLE INFO

Article history:

Received 24 June 2011

Received in revised form

4 November 2011

Accepted 8 November 2011

Available online 18 November 2011

Keywords:

Zircon

Electron backscatter diffraction

Plastic strain

Dislocation creep

Diffusion

Inclusion

Pore

ABSTRACT

A population of oscillatory zoned, igneous zircon grains in a Javanese andesite contains fluid and mineral inclusions (up to 10 μm across) trapped during zircon growth. Orientation contrast imaging and orientation mapping by electron backscatter diffraction reveal that crystal-plastic deformation overprints growth zoning and has localized around 1–10 μm pores and inclusions. Cumulative crystallographic misorientation of up to 25° around pores and inclusions in zircon is predominantly accommodated by low-angle (<5°) orientation boundaries, with few free dislocations in subgrain interiors. Low-angle boundaries are curved, with multiple orientation segments at the sub-micrometer scale. Misorientation axes associated with the most common boundaries align with the zircon c-axis and are consistent with dislocation creep dominated by <100>(010) slip. A distinctly different population of sub-micron pores is present along subgrain boundaries and their triple junctions. These are interpreted to have formed as a geometric consequence of dislocation interaction during crystal-plasticity. Dislocation creep microstructures are spatially related to differences in cathodoluminescence spectra that indicate variations in the abundance of CL-active rare earth elements. The extent of the modification suggests deformation-related fast-pathway diffusion distances that are over five orders of magnitude greater than expected for volume diffusion. This enhanced diffusion is interpreted to represent a combination of fast-diffusion pathways associated with creep cavitation, dislocations and along low-angle boundaries. These new data indicate that ductile deformation localised around inclusions can provide fast pathways for geochemical exchange. These pathways may provide links to the zircon grain boundary, thus negating the widely held assumption that inclusions in fracture-free zircon are geochemically armoured once they are physically enclosed.

Crown Copyright © 2011 Published by Elsevier Ltd. All rights reserved.

1. Introduction

The growth of zircon (ZrSiO_4) from a melt or in metamorphic rocks is commonly accompanied by entrapment or overgrowth of solid mineral phases, melt or fluid inclusions at the migrating zircon/matrix interface. Zircon from a wide range of igneous rock types contains inclusions, that have been used to reveal information about the magma composition from which the zircon grew, temperature conditions during zircon growth, and melt/zircon partition coefficients (Chupin et al., 1998; Danyushevsky et al., 2002;

Li, 1994; Thomas et al., 2003, 2002). The integration of petrological and geochemical studies of the inclusion mineralogy with U–Pb geochronology and trace element geochemistry of zircon permits petrogenetic processes to be placed within an absolute temporal framework. Such an approach can be valuable, for example, in constraining prograde metamorphic pressure–temperature–time paths that are otherwise difficult or impossible to access (Katayama and Maruyama, 2009; Katayama et al., 2002; Liu et al., 2004; Massonne and Nasdala, 2003). Significantly, the ability of zircon to resist chemical and physical breakdown allows old zircons to be used to constrain processes in the early Earth, for example to support the presence of volatile-rich granitoid magmas in the Archaean (Chupin et al., 1998), cool Hadean surface temperatures (Hopkins et al., 2010), and the operation of subduction as far back as 4.25 Ga (Menneken et al., 2007; Nemchin et al., 2008).

* Corresponding author. Tel.: +61 0 8 9266 4372.

E-mail address: n.timms@curtin.edu.au (N.E. Timms).

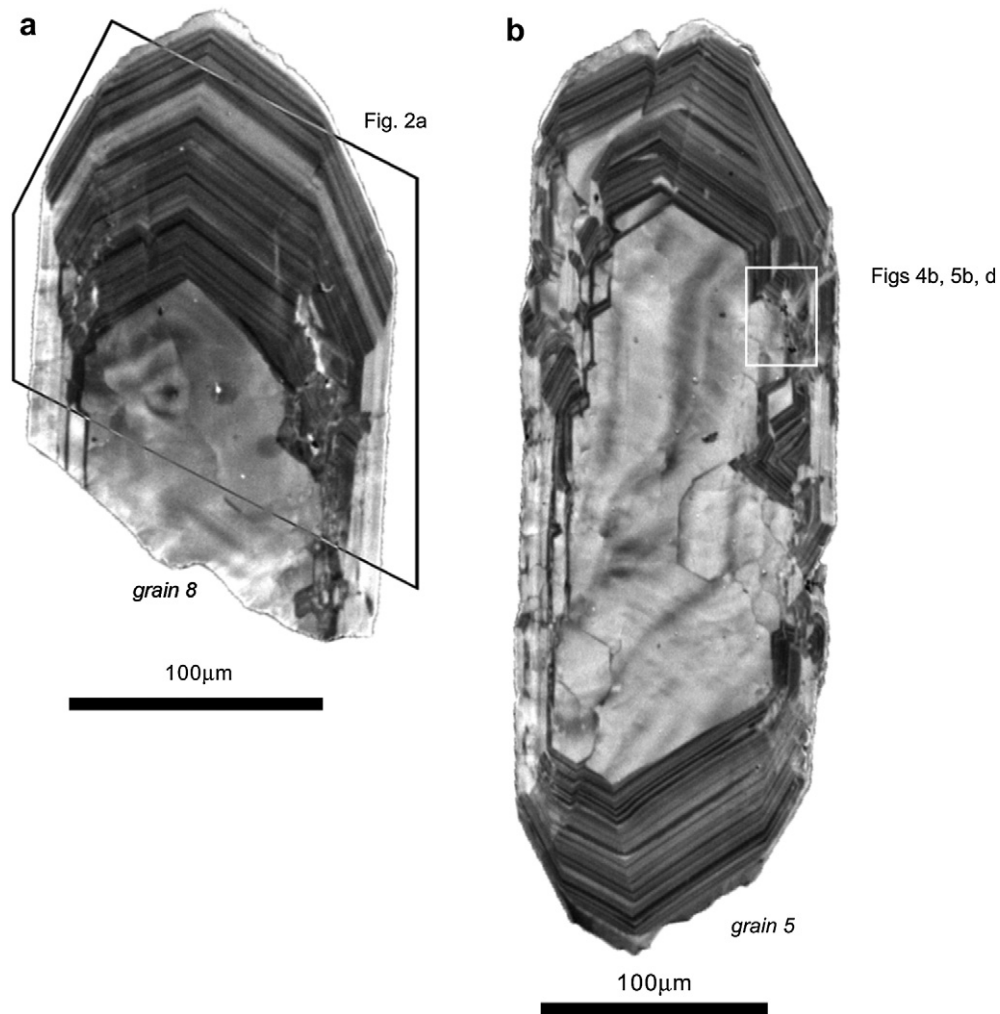


Fig. 1. (a) Panchromatic cathodoluminescence image of zircon grain 8 from the deformed magmatic population from sample Jhs2Pon4 showing cores and oscillatory zoned rim. (b) Panchromatic cathodoluminescence image of zircon grain 5.

Table 1
SEM and EBSD settings and statistics.

Technique	SEM	Detector/acquisition system	Acc. voltage (kV)	Probe current	Working distance (mm)	Tilt (degrees)
PCL	Phillips XL30 (W-filament)	KE developments	10	Spot 7	17.4	0
OCI	Zeiss Neon Dual FIB-FEG	Annular backscatter detector	30	50 pA	4.7–5.4	0
EBSD	Phillips XL30 (FEG)	Oxford instruments channel 5.9	20	Spot 5	20	70
FIB	Helios D433 Dual FIB-FEG	Helios	5/30	16 pA to 9.7 nA	4.5	52
λCL	JEOL 8530F FEG-EPMA	XCLent III	10	10 nA	fixed	0
EBSD settings		Fig. 4a, 5a,c		Fig. 4b, 5b, d		Fig. 6a
EBSP collection time per frame (ms)		60		60		60
Background (frames)		64		64		64
EBSP noise reduction (frames)		4		4		4
(binning)		4 × 4		4 × 4		4 × 4
(gain)		Low		Low		Low
Hough resolution		65		65		65
Match units		Zircon ^a		Zircon ^a , magnetite		Zircon ^a
Band detection – no. of bands		8		8		8
Step distance (μm)		0.1		0.1		1
Indexing (percent)		97.14		Zircon: 97.17, magnetite: 0.46		96
Data noise reduction – ‘wildspike’ removal		Yes		Yes		Yes
- nearest neighbour zero solution extrapolation		5		5		5

^a generated from zircon crystal structure at 9.8 Atm (~1 MPa) (Hazen and Finger, 1979).

Download English Version:

<https://daneshyari.com/en/article/4733393>

Download Persian Version:

<https://daneshyari.com/article/4733393>

[Daneshyari.com](https://daneshyari.com)